

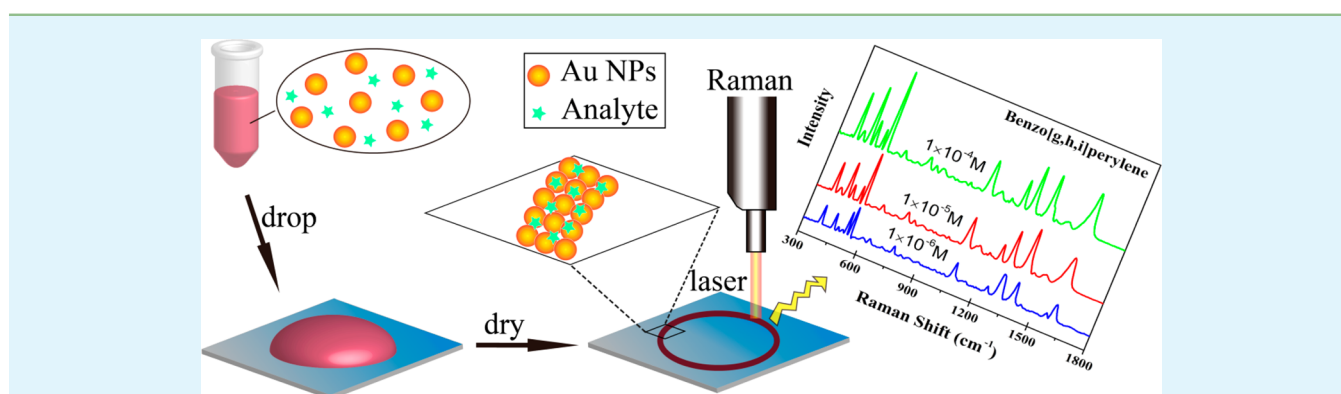
Facile Detection of Polycyclic Aromatic Hydrocarbons by a Surface-Enhanced Raman Scattering Sensor Based on the Au Coffee Ring Effect

Jianwei Xu,^{†,‡} Jingjing Du,[‡] Chuanyong Jing,^{*,‡} Yongli Zhang,^{*,†} and Jinli Cui[‡]

[†]College of Architecture and Environment, Sichuan University, Chengdu 610065, People's Republic of China

[‡]State Key Laboratory of Environmental Chemistry and Ecotoxicology, Research Center for Eco-Environmental Sciences (RCEES), Chinese Academy of Sciences (CAS), Beijing 100085, People's Republic of China

S Supporting Information



ABSTRACT: Surface-enhanced Raman scattering (SERS) analysis of environmental hydrophobic pollutants without chemical functionalization of a bare nanoparticle (NP) substrate presents a challenge. The motivation for our study is to develop a highly reproducible and robust portable SERS sensor for detection and identification of polycyclic aromatic hydrocarbons (PAHs) using bare Au NPs. Our hypothesis is that the coffee ring effect could separate PAHs from the bulk solution and concentrate them on the closely packed Au NP ring, consequently enhancing their Raman scattering. This premise was confirmed with the commonly used citrate-reduced Au NPs in 20 nm, having no structural uniqueness. Because of the coffee ring effect, however, closely packed but not aggregated Au NP arrays were formed and, consequently, facilitated the separation and concentration of hydrophobic PAHs. As a result, a prominent SERS enhancement can be obtained on the ring because of the electromagnetic mechanism. A mixture of six PAHs with different numbers of benzene rings, namely, naphthalene, anthracene, pyrene, benzo[*a*]pyrene, benzo[*g,h,i*]perylene, and indeno[1,2,3-*cd*]pyrene, could be readily identified in river water. This portable SERS sensor based on the coffee ring effect provides a robust and versatile approach in PAH detection without the need for stringent structural requirements for Au NPs.

KEYWORDS: SERS, coffee ring effect, Au nanoparticles, PAHs

INTRODUCTION

Surface-enhanced Raman scattering (SERS) is a rapid and ultrasensitive spectroscopic technique in chemical analysis, taking advantage of the explosive growth in nanofabrication.^{1–3} Great efforts have been made in the attempt to synthesize SERS-active noble metal nanoparticles (NPs) with tunable size, shape, and functionality. These NPs deposited on solid surfaces can form closely packed but non-aggregated arrays to promote substantial SERS enhancement.⁴ Thus, a broad diversity of techniques have been exploited to fabricate periodic and reproducible arrays, including spin-coating,⁵ electron beam lithography,⁶ vapor deposition,⁷ and self-assembly on functionalized surfaces.⁸ These techniques result in NPs with exceptional SERS enhancement and high reproducibility. However, stringent and laborious protocols and expensive

equipment are the two minimum prerequisites to reliably control the SERS substrate characteristics.^{9–11} Therefore, developing a facile and robust SERS sensor for environmental monitoring purposes motivates our research.

An intrinsic difficulty in environmental analysis is separating trace amounts of analytes from complex matrices, and this difficulty is also a factor in SERS implementation. For example, rigorous sample pretreatment is generally required before identification and quantification of polycyclic aromatic hydrocarbons (PAHs) using expensive instruments, including high-performance liquid chromatography (HPLC), gas chromatog-

Received: February 1, 2014

Accepted: April 10, 2014

Published: April 10, 2014

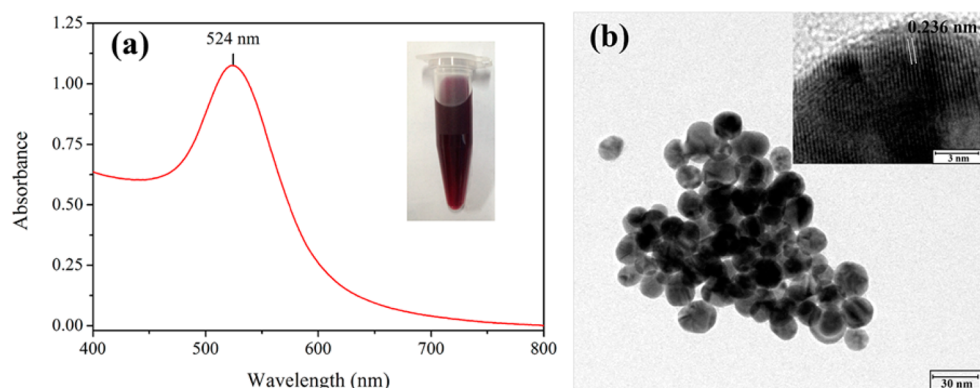


Figure 1. (a) UV–vis spectrum of the Au NPs. The inset shows a photograph of the Au NP colloid. (b) TEM and (inset) HR-TEM images of the Au NPs.

raphy (GC), and GC/mass spectrometry (MS). The SERS detection of PAHs is also a challenge because of the poor affinity of trace PAHs on NPs compared to the competing ions in the bulk solution.^{12,13} Therefore, modified NPs with new properties and functionalities are synthesized to capture PAHs to metal surfaces. The functional groups generally include calixarenes,¹⁴ viologen,¹⁵ humic acids,¹⁶ thiol groups,^{17,18} and cyclodextrin.¹⁹

Herein, we propose a practical approach integrating analyte separation and detection in one portable SERS platform using the well-known coffee ring effect.²⁰ The self-assembled coffee ring can separate and pre-concentrate analytes of interest because of the interplay of contact line pinning, solvent evaporation, and capillary flow.²¹ Thus, Raman analysis using the coffee ring pattern opens an avenue in bioanalytical research.^{22–26}

The objective of this study was to develop a rapid and reproducible SERS sensor for PAH detection and identification using the coffee ring effect. Our hypothesis is that the coffee ring effect could separate PAHs from the bulk solution and concentrate them on the closely packed Au NP ring, which consequently enhances their Raman scattering. To investigate the premise, the commonly used citrate-reduced Au NP was adopted in this study as the SERS substrate. The effectiveness of the SERS sensor was validated using a group of PAHs with different numbers of benzene rings, namely, naphthalene (NAP), anthracene (ANT), pyrene (PYR), benzo[*a*]pyrene (BaP), benzo[*g,h,i*]perylene (BPE), and indeno[1,2,3-*cd*]pyrene (IPY). This portable SERS sensor provides an easy and reliable measurement method for trace environmental pollutants.

EXPERIMENTAL SECTION

Chemicals and Materials. All reagents were of analytical reagent grade and used without further purification. Chloroauric acid tetrahydrate (HAuCl₄·4H₂O) and trisodium citrate dehydrate were purchased from Sinopharm Chemical Reagent Co., Ltd. (China). PAHs were obtained from J&K Scientific, Ltd. (China). Absolute ethanol (>99.7%) and methyl silicone oil (>97%) were from Beijing Chemical Reagents Company (China). Milli-Q water (>18.2 MΩ) was used in all experiments.

The PAH stock solutions (1 × 10^{−3} M) were prepared in acetone for BPE and in ethanol for other PAHs, and the PAH working solutions were obtained by diluting the stock solutions in water. Water from the Qing River was passed through a 0.45 μm membrane before use to prepare river water samples containing six PAHs. The stock solutions of NAP, ANT, PYR, BaP, BPE, and IPY were added to the

river water to reach final concentrations of each PAH of 1 × 10^{−5}, 5 × 10^{−6}, and 1 × 10^{−6} M.

Synthesis of Au NPs. All glassware and stirring paddles were rigorously cleaned with *aqua regia* (HCl/HNO₃ = 3:1, v/v), followed by thorough rinsing with Milli-Q water prior to use. Citrate-reduced monodispersed Au NPs were synthesized by modifying the standard sodium citrate method described in the literature.²⁷ Briefly, 1 mL of 2 wt % HAuCl₄ solution was mixed with 23 mL of water in a three-neck round-bottom flask and heated to 100 °C in an oil bath. Then, 1 mL of 50 mg/mL sodium citrate was added to the above solution and reacted for 15 min. Then, the mixture was allowed to cool to room temperature, and the obtained Au colloid solution was used within 48 h.

Treatment of Silicon Wafer. Hydrophilic and hydrophobic surface treatments on a silicon wafer were compared for the SERS enhancement. In the hydrophilic treatment, the silicon wafer was cleaned thoroughly with absolute ethanol under sonication for 30 min. In the hydrophobic treatment, the silicon wafer from the first treatment was polished with methyl silicone oil.

Sample Preparation for SERS Analysis. R6G samples (10 μL) in various concentrations were mixed with Au NPs (10 μL) prepared as described above. About 5 μL of the mixture was then dropped onto silicon wafer, and the SERS signal was collected.

PAH samples (10 μL) with various concentrations were mixed with Au NPs (10 μL). Then, 5 μL of the mixture was dropped onto the methyl silicone oil-treated silicon wafer and dried in the ambient environment. The SERS signal was collected at the ring deposition pattern after evaporation. A portable Raman spectrometer (Enwave Optronics, Inc., Irvine, CA) with a 4 cm^{−1} resolution at 785 nm excitation energy was used for the measurement at an integration time of 5 s.

Characterization. The ultraviolet–visible (UV–vis) spectrum of gold nanoparticles was collected on a Shimadzu UV-2550 spectrophotometer between 200 and 800 nm. The size and morphology of Au NPs were characterized using high-resolution transmission electron microscopy (HR-TEM, JEM-2010, JEOL). The surface morphology of the coffee ring pattern was obtained using field emission scanning electron microscopy (FESEM, SU-8020, Hitachi) with an Oxford energy-dispersive X-ray (EDX) analyzer. The SERS mapping of coffee ring patterns was measured using Renishaw InVia Raman microscopy equipped with a 785 nm laser line as the excitation source.

RESULTS AND DISCUSSION

Characterization of Au NPs. The burgundy Au colloids resulted in an absorption peak at 524 nm in the UV–vis spectrum (Figure 1a).²⁸ The ratio of peak intensity at this surface plasmon resonance (524 nm) to that at 450 nm was 1.77, suggesting the Au NP size of 23 nm.²⁹ In agreement with our UV–vis estimation, the TEM analysis resolved the average size of Au NPs at 20 nm (Figure 1b). Moreover, the inset HR-

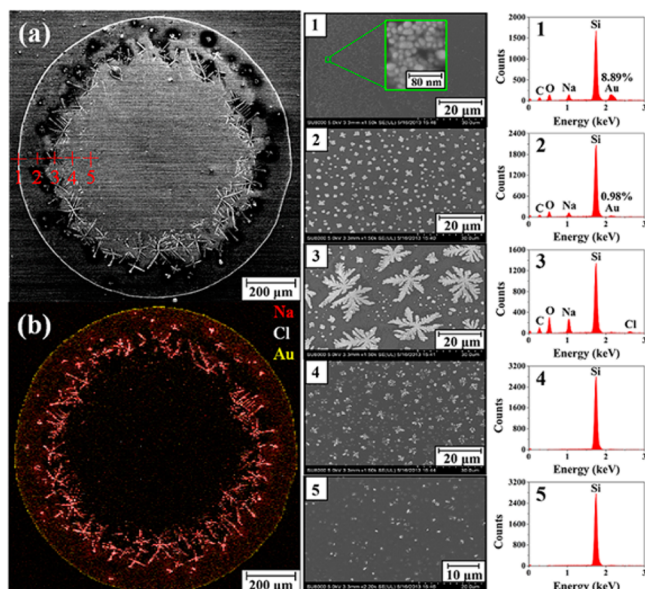


Figure 2. (a) SEM image and (b) EDX analysis for the coffee ring pattern (the red color represents Na; the white color represents Cl; and the yellow color represents Au). The middle column shows the SEM images, and the right column is the EDX results for five points along the diameter.

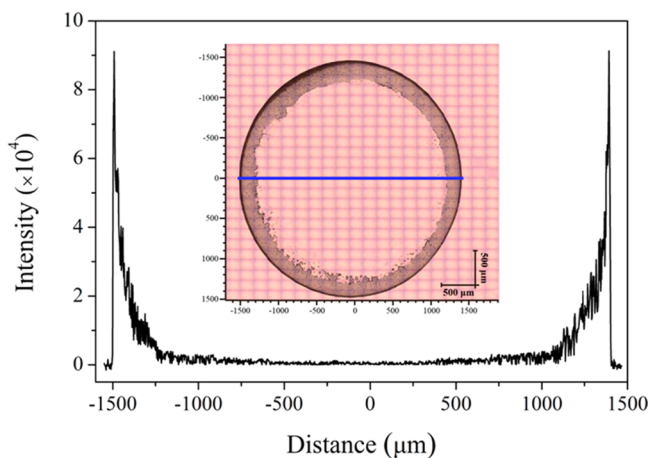


Figure 3. SERS intensity of BaP at 610 cm^{-1} along the diameter of the ring. The inset shows the white light image of the coffee ring pattern formed by a $5\text{ }\mu\text{L}$ drop of the mixture of Au NPs and $1 \times 10^{-5}\text{ M}$ BaP.

TEM image reveals the lattice fringe spacing of 0.236 nm , corresponding to the distance between the Au (111) crystal planes.³⁰ The characterization results suggest that no structural uniqueness can be found in the obtained Au NPs using the routine synthesis approach. The Au NP colloid, as expected, was effective in detecting the probe molecule, R6G (see Figure S4 of the Supporting Information). However, this colloid cannot generate any SERS signals for PAHs (see Figure S4 of the Supporting Information). Thus, such an Au NP colloid can be a good example to verify whether the SERS enhancement because of the coffee ring effect can be used as a versatile approach without the need for a stringent structural requirement for the NPs.

Coffee Ring Patterns. After a $5\text{ }\mu\text{L}$ drop of PAH and Au NP mixture evaporated on a hydrophobic surface, a readily visible ring pattern was formed, as evidenced by the SEM image (Figure 2a). The elemental mapping results (Figure 2b) clearly

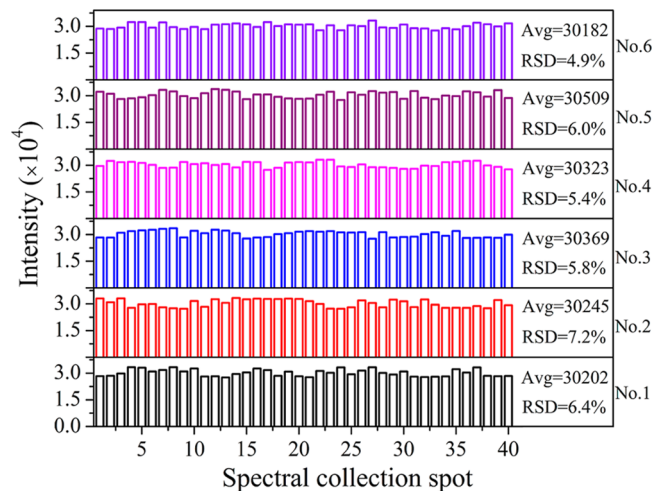


Figure 4. SERS intensity of $5 \times 10^{-6}\text{ M}$ BaP collected at 40 randomly chosen spots along the edge of six coffee ring samples. The average SERS intensity (Avg) and relative standard deviation (RSD) of 40 spots for each coffee ring samples are also summarized.

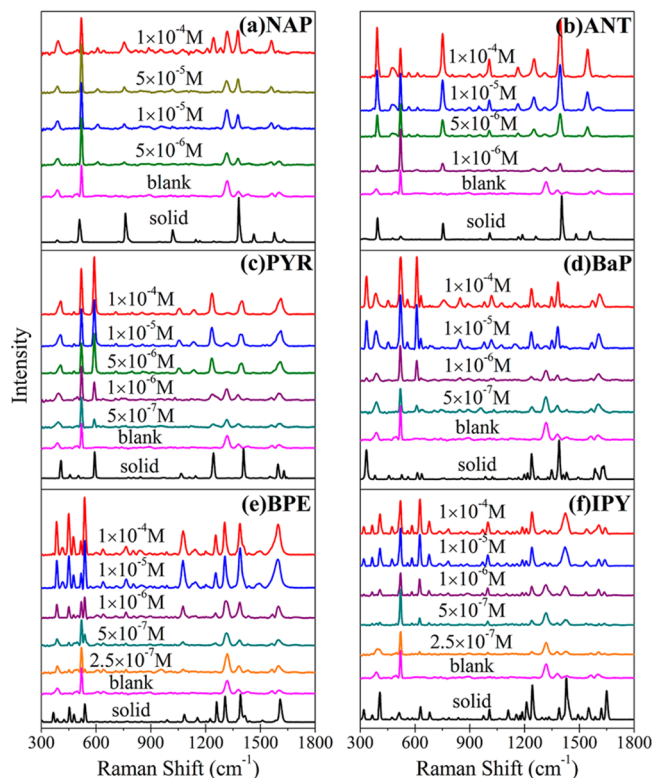
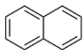
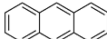

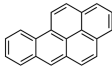

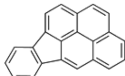


Figure 5. Representative Raman spectra of typical PAHs with different concentrations measured at the edge of the coffee ring pattern: (a) naphthalene, (b) anthracene, (c) pyrene, (d) benzo[*a*]pyrene, (e) benzo[*g,h,i*]perylene, and (f) indeno[1,2,3-*cd*]pyrene.

show that Au NPs deposited and formed the periphery of the ring, whereas the bare silicon wafer was detected in the center of the ring, with NaCl primarily in between. NaCl was the residue from the synthesis of Au NPs. Further EDX analysis at spots 1–5 along the diameter (Figure 2) confirms that the soluble NaCl was left inward, whereas carbon and Au NPs were on the ring. This separation of analytes based on their solubility and hydrophobicity during the ring formation has been used in Raman analysis of biomedical samples.^{31,32} When a drop

Table 1. Molecular Structure, K_{ow} , Detection Limit of PAHs, Peak Position for Quantitative Analysis, and Calculation of the Enhancement Factor

PAHs		$\log K_{ow}$ ⁴⁰	Conc.(μ M)	Peak (cm^{-1})	EF ^a
Naphthalene (NAP)		3.32	5	1378	5×10^3
Anthracene (ANT)		4.20	1	751	2.5×10^3
Pyrene (PYR)		5.20	0.5	592	3×10^4
Benzo(a)pyrene (BaP)		6.20	0.5	610	1×10^5
Benzo(g,h,i)perylene (BPE)		6.50	0.25	538	1×10^5
Indeno(1,2,3-cd)pyrene (IPY)		6.58	0.25	626	1.5×10^5

^aEnhancement factor was calculated by the following equation:^{12,39} $EF = (I_{SERS}/I_{RS})(C_{RS}/C_{SERS})$, where I_{SERS} is the SERS intensities of the most intense band for PAHs, I_{RS} is the normal Raman signal for the corresponding band of the neat PAHs, and C_{RS}/C_{SERS} is the concentration ratio of the PAHs in neat solution and on the SERS sample.

evaporates on a hydrophobic surface, the least soluble component starts to deposit at the periphery of the drop.³¹ Because PAH is hydrophobic and least soluble in the system, the carbon on the ring should come from PAH rather than sodium citrate.

Interestingly, the Au NPs on the ring were closely packed but not aggregated (Figure 2). This array should lead to high SERS enhancement because of the plasmon resonance of the closely connected Au NPs with the field enhancement within them.¹² Thus, the coffee ring effect could be used to separate and concentrate less soluble and hydrophobic PAHs and Au NPs to the fringe of the ring to generate the optimum conditions for SERS analysis.

SERS Enhancement. To explore the SERS enhancement along the Au ring, the intensity of the characteristic BaP peak at 610 cm^{-1} was measured along the diameter (Figure 3). Appreciable Raman intensity was observed on the ring and was immediately reduced to almost zero when sampling off the ring. This observation is in agreement with the distribution of PAHs and Au NPs (Figure 2).

The effect of hydrophilic and hydrophobic surface treatments on a silicon wafer was also studied. The droplets on hydrophilic and hydrophobic surfaces exhibited varying contact angles (see Figure S1 of the Supporting Information): β (hydrophobic) $>$ θ (hydrophilic). Hydrophobic surfaces concentrate particles more effectively than hydrophilic surfaces, resulting in uniformly smaller ring diameters (see Figure S2 of the Supporting Information). The primary underlying mechanism that describes this response is the liquid–surface contact area and the corresponding pinning perimeter. The condensed Au NPs on the ring on the oil-polished wafer facilitated the SERS enhancement, as evidenced by the 3-fold higher SERS peak intensity (see Figure S3 of the Supporting Information).

To study the reproducibility and uniformity of the Au ring, six replicate rings were prepared using $5 \times 10^{-6} \text{ M}$ BaP and Au NPs and SERS signals were collected at 40 spots randomly chosen along each ring. The peak intensities at 610 cm^{-1} for each sampling spot are shown in Figure 4. No statistically significant difference existed among the six Au rings ($p > 0.4$; see Table S1 of the Supporting Information) and among 40 different sampling locations on the same ring ($p > 0.4$; see Table S2 of the Supporting Information). The results demonstrate that the Au NP ring is a reproducible and uniform SERS substrate.

SERS Detection of PAHs. Six PAHs, including NAP, ANT, PYR, BaP, BPE, and IPY, were analyzed with SERS, and their spectra and peak assignments are shown in Figure 5 and Tables S3–S8 of the Supporting Information, respectively. For comparison purposes, spectra of the PAH standards and blank substrate were also collected. The substrate itself displayed four weak bands at 387, 1318, 1380, and 1602 cm^{-1} that may be attributable to citrate and its decomposition products.³³ Nevertheless, the background peaks would not interfere with the detection of the six PAHs (Figure 5).

In line with previous reports^{34–37} and our DFT calculations (see Figures S5–S10 of the Supporting Information), the observed SERS spectra agreed well with the corresponding Raman spectra for PAH standards (see Tables S3–S8 of the Supporting Information). The lack of change in SERS peaks from the Raman spectra implies that the enhancement may be mainly due to the electromagnetic mechanism, which does not require the formation of chemical bonds between the analyte and substrate.³⁸ The closely packed nanoparticles and nanogaps on the coffee ring resulted in pronounced SERS enhancement for molecules within them.

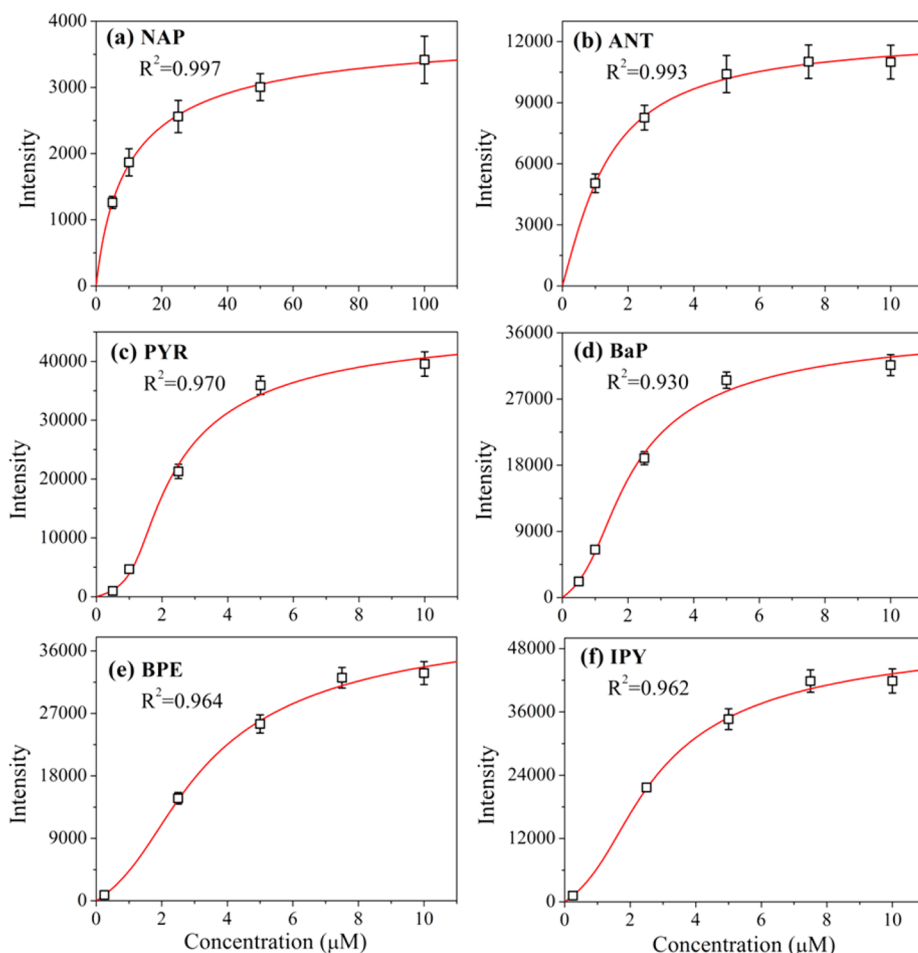


Figure 6. Calibration curves for (a) NAP, (b) ANT, (c) PYR, (d) Bap, (e) BPE, and (f) IPY using the most intense SERS band. The data points represent the average \pm standard deviation for 50 randomly chosen points at the edge of four rings. Signal collection time = 5 s.

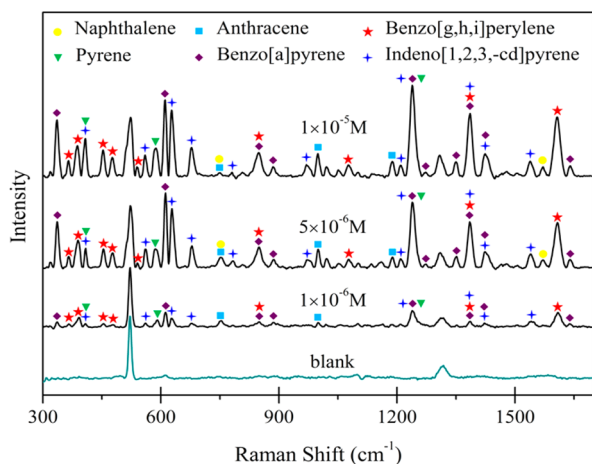


Figure 7. SERS spectra of PAHs in Qing River water spiked with six PAHs at 1×10^{-5} , 5×10^{-6} , and 1×10^{-6} M concentration levels for each PAH.

The detection limit and enhancement factor (EF) estimated using the most intense band³⁹ for each PAH were a function of its octanol–water partition coefficient, K_{ow} (Table 1). In agreement with our previous report,¹⁸ the hydrophobic forces, as indicated with K_{ow} , facilitate the PAHs concentrating on the edge of the Au ring, whereas soluble ions are left in the center.

Quantitative SERS Analysis of PAHs. To quantify the SERS response as a function of the PAH concentration, the SERS intensity at the most intense PAH band was recorded from 50 randomly selected spots on the ring, and the results are listed in Table 1 and Figure 6. The concentration-dependent response can be well-described using the following equation:

$$\frac{I}{c} = P + QI + RI^2 \quad (1)$$

where I is the SERS intensity of each PAH at the most intense Raman band, c is the concentration of each PAH, and P , Q , and R are the fitting parameters. The signal intensity increased in response to the increasing PAH concentration and then reached a plateau, probably because of saturation of the “hot spots” of the SERS substrate. A similar relationship between the PAH concentration and SERS intensity was also observed by Kwon et al.³⁴

Identification of PAH Mixtures. The SERS spectra of a sample containing six PAHs in river water matrices were collected as shown in Figure 7. The key SERS peaks of the individual PAHs can be distinguished, where the discriminant peaks of each PAH are labeled with different symbols (Figure 7). These peaks can be used to rapidly screen PAHs in complex river water matrices. A general leveling off of the SERS intensity with the concentration was observed because the six PAH molecules compete for the available “hot spots” of the Au NPs.

CONCLUSION

The present work has demonstrated a robust and effective SERS sensor based on the coffee ring effect for the rapid detection and identification of environmental hydrophobic pollutants. The Au NPs synthesized using a routine preparation protocol form a highly reproducible and robust ring pattern, resulting in closely packed but not aggregated Au NP arrays. This coffee ring effect facilitates the separation and concentration of the hydrophobic PAHs. As a result, prominent SERS enhancement can be obtained because of the electromagnetic mechanism. Specifically, the present approach could detect the target analytes, which is a challenge for direct SERS detection using bare Au NPs because of their poor affinity with Au NPs without functional modification. Hence, the present method should have great application in the rapid identification and quantification of hydrophobic pollutants in the environment.

ASSOCIATED CONTENT

Supporting Information

Statistic results of reproducibility and uniformity tests and experimental and density functional theory (DFT)-calculated Raman frequencies. This material is available free of charge via the Internet at <http://pubs.acs.org>.

AUTHOR INFORMATION

Corresponding Authors

*Telephone/Fax: +86-10-6284-9523. E-mail: cjying@rcees.ac.cn.

*E-mail: zxm581212@163.com.

Notes

The authors declare no competing financial interest.

ACKNOWLEDGMENTS

The authors acknowledge the financial support of the National Basic Research Program of China (2014CB114402), the National Natural Science Foundation of China (41023005, 21307147, and 21321004), and Research Center for Eco-Environmental Sciences (RCEES) (YSW2013A01).

REFERENCES

- (1) Tan, E.-Z.; Yin, P.-G.; You, T.-t.; Wang, H.; Guo, L. Three dimensional design of large-scale TiO₂ nanorods scaffold decorated by silver nanoparticles as SERS sensor for ultrasensitive malachite green detection. *ACS Appl. Mater. Interfaces* **2012**, *4*, 3432–3437.
- (2) Kim, K.; Lee, J. W.; Shin, K. S. Polyethylenimine-capped Ag nanoparticle film as a platform for detecting charged dye molecules by surface-enhanced Raman scattering and metal-enhanced fluorescence. *ACS Appl. Mater. Interfaces* **2012**, *4*, 5498–5504.
- (3) Lee, C. H.; Tian, L.; Singamaneni, S. Paper-based SERS swab for rapid trace detection on real-world surfaces. *ACS Appl. Mater. Interfaces* **2010**, *2*, 3429–3435.
- (4) Fan, M.; Andrade, G. F.; Brolo, A. G. A review on the fabrication of substrates for surface enhanced Raman spectroscopy and their applications in analytical chemistry. *Anal. Chim. Acta* **2011**, *693*, 7–25.
- (5) Li, D.; Lee, J. Y.; Kim, D. H. Responsive polymer/gold nanoparticle composite thin films fabricated by solvent-induced self-assembly and spin-coating. *J. Colloid Interface Sci.* **2011**, *354*, 585–591.
- (6) Yue, W.; Wang, Z.; Yang, Y.; Chen, L.; Syed, A.; Wong, K.; Wang, X. Electron-beam lithography of gold nanostructures for surface-enhanced Raman scattering. *J. Microchem. Microeng.* **2012**, *22*, 125007.
- (7) Asiala, S. M.; Schultz, Z. D. Characterization of hotspots in a highly enhancing SERS substrate. *Analyst* **2011**, *136*, 4472–4479.
- (8) Su, Q.; Ma, X.; Dong, J.; Jiang, C.; Qian, W. A reproducible SERS substrate based on electrostatically assisted APTES-functionalized

surface-assembly of gold nanostars. *ACS Appl. Mater. Interfaces* **2011**, *3*, 1873–1879.

(9) Kho, K. W.; Shen, Z. X.; Zeng, H. C.; Soo, K. C.; Olivo, M. Deposition method for preparing SERS-active gold nanoparticle substrates. *Anal. Chem.* **2005**, *77*, 7462–7471.

(10) Eshkeiti, A.; Narakathu, B.; Reddy, A.; Moorthi, A.; Atashbar, M.; Rebrosova, E.; Rebroso, M.; Joyce, M. Detection of heavy metal compounds using a novel inkjet printed surface enhanced Raman spectroscopy (SERS) substrate. *Sens. Actuators, B* **2012**, *171*, 705–711.

(11) Qu, L.-L.; Li, D.-W.; Xue, J.-Q.; Zhai, W.-L.; Fossey, J. S.; Long, Y.-T. Batch fabrication of disposable screen printed SERS arrays. *Lab Chip* **2012**, *12*, 876–881.

(12) Jiang, X.; Lai, Y.; Yang, M.; Yang, H.; Jiang, W.; Zhan, J. Silver nanoparticle aggregates on copper foil for reliable quantitative SERS analysis of polycyclic aromatic hydrocarbons with a portable Raman spectrometer. *Analyst* **2012**, *137*, 3995–4000.

(13) López-Tocón, I.; Otero, J. C.; Arenas, J. F.; García-Ramos, J. V.; Sánchez-Cortés, S. Trace detection of triphenylene by surface enhanced Raman spectroscopy using functionalized silver nanoparticles with bis-acridinium lucigenine. *Langmuir* **2010**, *26*, 6977–6981.

(14) Kwon, Y. H.; Sowoidnich, K.; Schmidt, H.; Kronfeldt, H. D. Application of calixarene to high active surface-enhanced Raman scattering (SERS) substrates suitable for in situ detection of polycyclic aromatic hydrocarbons (PAHs) in seawater. *J. Raman Spectrosc.* **2012**, *43*, 1003–1009.

(15) Lopez-Tocon, I.; Otero, J. C.; Arenas, J. F.; Garcia-Ramos, J. V.; Sanchez-Cortes, S. Multicomponent direct detection of polycyclic aromatic hydrocarbons by surface-enhanced Raman spectroscopy using silver nanoparticles functionalized with the viologen host lucigenin. *Anal. Chem.* **2011**, *83*, 2518–2525.

(16) Qu, L. L.; Li, Y. T.; Li, D. W.; Xue, J. Q.; Fossey, J. S.; Long, Y. T. Humic acids-based one-step fabrication of SERS substrates for detection of polycyclic aromatic hydrocarbons. *Analyst* **2013**, *138*, 1523–1528.

(17) Gu, X. F.; Tian, S.; Zhou, Q.; Adkins, J.; Gu, Z. M.; Li, X. W.; Zheng, J. W. SERS detection of polycyclic aromatic hydrocarbons on a bowl-shaped silver cavity substrate. *RSC Adv.* **2013**, *3*, 25989–25996.

(18) Du, J.; Jing, C. Preparation of thiol modified Fe₃O₄@Ag magnetic SERS probe for PAHs detection and identification. *J. Phys. Chem. C* **2011**, *115*, 17829–17835.

(19) Xie, Y. F.; Wang, X.; Han, X. X.; Song, W.; Ruan, W. D.; Liu, J. Q.; Zhao, B.; Ozaki, Y. Selective SERS detection of each polycyclic aromatic hydrocarbon (PAH) in a mixture of five kinds of PAHs. *J. Raman Spectrosc.* **2011**, *42*, 945–950.

(20) Deegan, R. D.; Bakajin, O.; Dupont, T. F.; Huber, G.; Nagel, S. R.; Witten, T. A. Capillary flow as the cause of ring stains from dried liquid drops. *Nature* **1997**, *389*, 827–829.

(21) Bhardwaj, R.; Fang, X.; Somasundaran, P.; Attinger, D. Self-assembly of colloidal particles from evaporating droplets: Role of DLVO interactions and proposition of a phase diagram. *Langmuir* **2010**, *26*, 7833–42.

(22) Filik, J.; Stone, N. Drop coating deposition Raman spectroscopy of protein mixtures. *Analyst* **2007**, *132*, 544–550.

(23) Barman, I.; Dingari, N. C.; Kang, J. W.; Horowitz, G. L.; Dasari, R. R.; Feld, M. S. Raman spectroscopy-based sensitive and specific detection of glycosylated hemoglobin. *Anal. Chem.* **2012**, *84*, 2474–2482.

(24) Djaoued, Y.; Balaji, S.; Priya, S. Non-resonance micro-Raman spectroscopic studies on crystalline domoic acid and its aqueous solutions. *Spectrochim. Acta, Part A* **2007**, *67*, 1362–1369.

(25) Filik, J.; Stone, N. Investigation into the protein composition of human tear fluid using centrifugal filters and drop coating deposition Raman spectroscopy. *J. Raman Spectrosc.* **2009**, *40*, 218–224.

(26) Halvorson, R. A.; Vikesland, P. J. Drop coating deposition Raman (DCDR) for microcystin-LR identification and quantitation. *Environ. Sci. Technol.* **2011**, *45*, 5644–5651.

(27) Maiorano, G.; Sabella, S.; Sorce, B.; Brunetti, V.; Malvindi, M. A.; Cingolani, R.; Pompa, P. P. Effects of cell culture media on the

dynamic formation of protein–nanoparticle complexes and influence on the cellular response. *ACS Nano* **2010**, *4*, 7481–7491.

(28) Ghosh, S. K.; Pal, T. Interparticle coupling effect on the surface plasmon resonance of gold nanoparticles: From theory to applications. *Chem. Rev.* **2007**, *107*, 4797–4862.

(29) Haiss, W.; Thanh, N. T.; Aveyard, J.; Fernig, D. G. Determination of size and concentration of gold nanoparticles from UV–vis spectra. *Anal. Chem.* **2007**, *79*, 4215–4221.

(30) Ojea-Jiménez, I.; López, X.; Arbiol, J.; Puentes, V. Citrate-coated gold nanoparticles as smart scavengers for mercury(II) removal from polluted waters. *ACS Nano* **2012**, *6*, 2253–2260.

(31) Filik, J.; Stone, N. Analysis of human tear fluid by Raman spectroscopy. *Anal. Chim. Acta* **2008**, *616*, 177–184.

(32) Filik, J.; Stone, N. Investigation into the protein composition of human tear fluid using centrifugal filters and drop coating deposition Raman spectroscopy. *J. Raman Spectrosc.* **2009**, *40*, 218–224.

(33) Munro, C.; Smith, W.; Garner, M.; Clarkson, J.; White, P. Characterization of the surface of a citrate-reduced colloid optimized for use as a substrate for surface-enhanced resonance Raman scattering. *Langmuir* **1995**, *11*, 3712–3720.

(34) Kwon, Y. H.; Sowoidnich, K.; Schmidt, H.; Kronfeldt, H. D. Application of calixarene to high active surface-enhanced Raman scattering (SERS) substrates suitable for in situ detection of polycyclic aromatic hydrocarbons (PAHs) in seawater. *J. Raman Spectrosc.* **2012**, *43*, 1003–1009.

(35) Jones, C. L.; Bantz, K. C.; Haynes, C. L. Partition layer-modified substrates for reversible surface-enhanced Raman scattering detection of polycyclic aromatic hydrocarbons. *Anal. Bioanal. Chem.* **2009**, *394*, 303–311.

(36) Sun, B.; Dreger, Z.; Gupta, Y. High-pressure effects in pyrene crystals: Vibrational spectroscopy. *J. Phys. Chem. A* **2008**, *112*, 10546–10551.

(37) Onchoke, K. K.; Hadad, C. M.; Dutta, P. K. Structure and vibrational spectra of mononitrated benzo[*a*]pyrenes. *J. Phys. Chem. A* **2006**, *110*, 76–84.

(38) Du, J.; Cui, J.; Jing, C. Rapid in situ identification of arsenic species using a portable Fe₃O₄@Ag SERS sensor. *Chem. Commun.* **2014**, *50*, 347–349.

(39) Le Ru, E.; Blackie, E.; Meyer, M.; Etchegoin, P. Surface enhanced Raman scattering enhancement factors: A comprehensive study. *J. Phys. Chem. C* **2007**, *111*, 13794–13803.

(40) Zhang, Y.-F.; Ma, Y.; Gao, Z.-X.; Dai, S.-G. Predicting the cross-reactivities of polycyclic aromatic hydrocarbons in ELISA by regression analysis and CoMFA methods. *Anal. Bioanal. Chem.* **2010**, *397*, 2551–2557.